Histol Histopathol (1998) 13: 337-346

Histology and Histopathology

Morphological studies of glomeruli in obstructive kidneys by confocal laser scanning microscopy and quick-freezing replica method

A. Matsuda[1], N. Terada[2], H. Ueda[2], Y. Fujii[2], K. Tago[1], A. Ueno[1] and S. Ohno[2]
Departments of [1]Urology and [2]Anatomy, Yamanashi Medical University, Tamaho, Yamanashi, Japan

Summary. Morphological changes of glomeruli in obstructive kidneys were studied by using confocal laser scanning microscopy (CLSM), and quick-freezing and deep-etching (QF-DE) method. Twenty-one rabbits were divided into three groups, consisting of control, 6-hr bilateral ureteral obstruction (BUO) and 24-hr BUO. In the experimental groups, the attenuation of cell bodies, the lengthening and stretching of major processes, the cystic formation in the cytoplasm and the fusion of foot processes were observed on conventional ultrathin sections. These changes in the 24-hr BUO group were more clearly observed than those in the 6-hr BUO group. By the CLSM, cell bodies and foot processes of podocytes in the experimental groups were more intensely immunostained with anti-α-tubulin antibody and phalloidin-FITC. By the QF-DE method, cytoskeletons in the podocyte cell bodies and major processes were composed of numerous intermediate filaments, but distinct changes of actin filaments and microtubules were not observed in the control and experimental groups. Considering the physiological changes in BUO, the mechanical stress appeared to be brought about by hemodynamic factors rather than the change of intratubular pressure, resembling the morphological changes in experimental animals with hyperfiltration and the homeostatic adaptation of podocytes under the BUO condition.

Key words: Podocyte, Cytoskeleton, Obstructive kidney, Confocal laser microscopy, Quick-freezing

Introduction

It has been reported that glomerular podocytes undergo dramatical changes in response to experimental conditions and renal diseases, which are assumed to play an important role in glomerular sclerosis (Elema and Arends, 1975; Olson et al., 1985; Andrews, 1988; Frise et al., 1989; Nagata and Kriz, 1992; Nagata et al., 1992). Some studies have indicated that direct cell toxicity (Elema and Arends, 1975; Frise et al., 1989) and mechanical stress (Nagata and Kriz, 1992; Nagata et al., 1992) are two main factors which injure glomerular podocytes. In the case of obstructive kidneys, there is a progressive fall in glomerular filtration rate (GFR) due to an increase of intratubular pressure at first and then to a decrease of renal plasma flow (RPF) following a ureteral obstruction (Klahr and Harris, 1992). So the hemodynamic changes are supposed to cause the glomerular damage as a mechanical stress. However, there are a few studies about morphological changes of podocytes in the obstructive kidneys (Kamiya, 1968; Nagle et al., 1973; Nagle and Bulger, 1978; McDougal, 1990), which indicate fusion of foot processes as revealed by transmission electron microscopy (TEM). Moreover, a question still remains: how do podocytes respond to the hemodynamic changes in obstructive kidneys?

The way in which podocytes counteract the mechanical stress seems to be deeply related to their cytoskeletons. It is well known that three main components of cytoskeletons are actin filaments, intermediate filaments and microtubules. The actin filaments exist mainly in foot processes to regulate the rate of solute efflux across the glomerular wall (Andrews, 1988). On the contrary, cytoskeletons in cell bodies and major processes consist of microtubules and intermediate filaments to maintain the cell shape. However, it has not yet been clearly shown that such different distinction in the distribution of these filaments plays an important role in glomerular functions (Bachmann et al., 1983; Andrews, 1988; Drenckhahn and Franke, 1988).

Recently, confocal laser scanning microscopy (CLSM) has often been used to fulfill a decrease of background noise (White et al., 1987). So CLSM makes it possible to obtain a clear image of any given focus plane with higher resolution than conventional immunofluorescence imaging. Moreover, the quick-freezing and deep-etching (QF-DE) method, which is one of the new techniques in electron microscopy, has an

Offprint requests to: Dr. Akira Matsuda, M.D., Department of Urology, Yamanashi Medical University, 1110 Shimokato, Tamaho, Yamanashi, 409-38, Japan

advantage for an examination of three-dimensional ultrastructures of glomerular tissues at higher resolution (Ohno et al., 1992). Recently, the QF-DE method has often been applied ot routine morphological analyses in order to examine pathological changes in some renal diseases (Naramoto et al., 1991a,b).

In this study, we investigated cytoskeletal changes of glomerular podocytes during the time course of obstructive rabbit kidneys. To examine the cytoskeletons in the podocytes, we used both CLSM and QF-DE method in addition to conventional electron microscopy.

Materials and methods

Twenty-one male Japanese white rabbits, weighing about 2 kg, were used in this study. They were divided into three groups, consisting of control, 6-hr bilateral ureteral obstruction (BUO) and 24-hr BUO. In both BUO groups, the rabbits were anesthetized with an intravenous injection of sodium pentobarbital (25 mg/kg). The abdomen was opened through low middle-line incision, and bilateral ureters were ligated with silk sutures at the vesicoureteral junction. After the abdomen was closed, they were returned to their cages, and allowed free access to standard chow and water. In the control group, the sham operation was done under the same condition.

The rabbits were anesthetized 6 or 24 hours after the operation time and their abdomen was opened again. The renal perfusion fixation was performed through a 23-gauge needle put into the abdominal aorta. The perfusion pressure was about 160cmH_2O. First, the kidneys were perfused with 2% paraformaldehyde containing 10 μM Taxol (Sigma chemical Co, St. Louis, MO, USA), and the right kidney was removed for light microscopy (LM), immunofluorescent microscopy (IM), and quick-freezing and deep-etching (QF-DE) method. Following an additional perfusion with 2.5% glutaraldehyde, the left kidney was taken out for conventional electron microscopy (EM). Some parts of the right renal cortex were cut into small pieces and washed in 0.1M phosphate buffer (PB), pH 7.3 containing 10 μM Taxol for 30 min to remove soluble proteins (Ohno et al., 1992). These tissues were postfixed with 0.25% gltuaraldehyde in PB for 30 min. After washing with PB, they were processed for QF-DE method.

Other tissue blocks were fixed again with 2% paraformaldehyde in PB containing 10 μM Taxol at 4 °C overnight, and then washed in PB for LM and IM. For LM, they were routinely embedded in paraffin, and sections were cut at 3 μm thickness and stained with hematoxylin-eosin. For IM, after cortical tissues of the right kidney had been cut into small pieces, they were immersed in 20% sucrose and 10% glycerol in PB, buried in OCT compound and frozen in liquid nitrogen. They were sectioned at 10 μm thickness in a cryostat and then treated with 0.5% saponin in PB for 30 min to allow the antibody penetration.

(i) Conventional ultrathin sections

Cortical tissues of the left kidney were cut into small pieces with razor blades, fixed again in 2.5% glutaraldehyde in PB for an additional 2 hours and postfixed with 1% osmium tetroxide in PB at 4 °C for 1 hour. They were dehydrated in a graded series of ethanol and embedded in Epon 812. Ultrathin sections were cut with glass knives and stained with uranyl acetate and lead citrate, and then examined under a Hitachi H-600 electron microscope at 75kV.

(ii) Immunofluorescence staining

Some cryostat sections were treated with 10% rabbit whole serum in phosphate-buffered saline (PBS) for 1 hour. They were rinsed in PBS and incubated with monoclonal anti-α-tubulin antibody (Sanbio, bv., Am, Uden, Netherland) diluted at 1/10 in PBS for 1 hour. They were rinsed in PBS and incubated with rabbit anti-

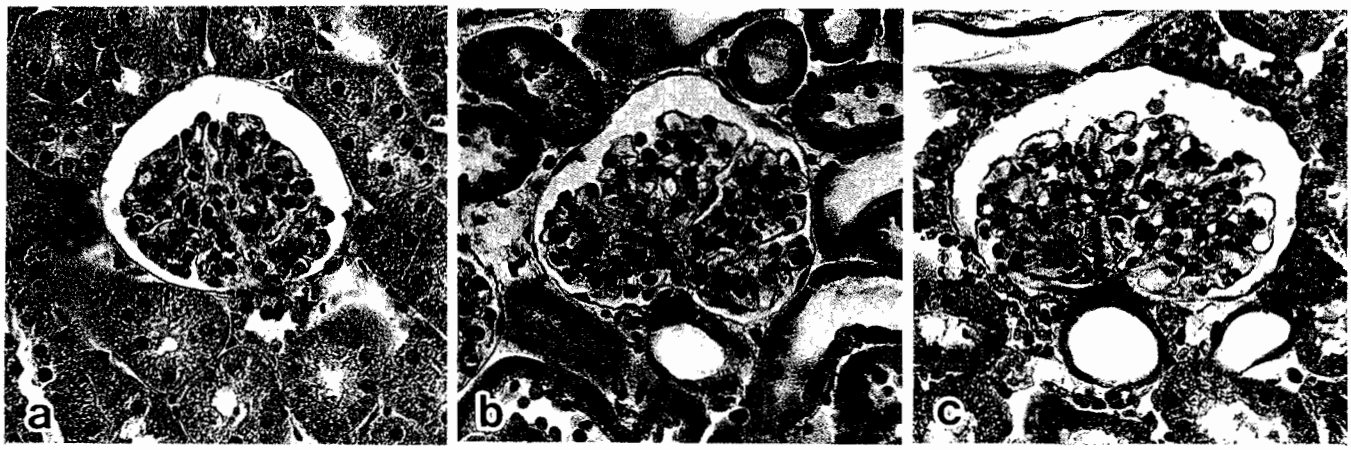

Fig. 1. Light micrographs of a typical glomerulus in the control **(a)**, 6-hr BUO **(b)** and 24-hr BUO groups **(c)**. HE staining. x 100

mouse IgG coupled with FITC (Cappel Laboratories, Inc., Dowingtown, PA, USA) diluted at 1/100 in PBS for 1 hour. Other sections were pre-treated in the same way and incubated with monoclonal anti-vimentin antibody (Boehringer Mannheim, GmbH. Mannheim, Germany) diluted at 1/10 in PBS for 1 hour. They were adequately washed in PBS and incubated with the secondary antibody as described in the previous sentences. As an immunostaining control, cryostat sections were incubated with normal mouse serum instead of each primary antibody and prepared in the same way. To identify actin filaments, other sections were incubated with phalloidin-FITC (Sigma Chemical Co.) diluted at 1/100 in PBS for 1 hour, washed in PBS for 1 hour and routinely mounted on slide glasses. All of them were observed with a confocal laser scanning microscope, Olympus LSM-GB 200.

(III) Quick-freezing and deep-etching method

The prepared tissues were immersed in 10% methanol and quickly frozen by a JFD-RFA freezing machine (JEOL Co., Tokyo, Japan) cooled with liquid nitrogen (-196 °C). They were transferred into liquid nitrogen and carefully freeze-fractured with a scalpel, as reported before (Ohno et al., 1992). The frozen specimens were put into an Eiko FD-3AS machine (Eiko Engineering Co., Ibaraki, Japan) and deeply etched under the vacuum conditions of $2\text{-}6\text{x}10^{-7}$ Torr at -95 °C for 15-20 min. The deeply etched tissues were rotary shadowed with platinum and carbon, as reported before (Ohno et al., 1992). The replica membranes with the specimens were taken out and immediately coated with 2% collodion. Moreover, the kidney tissues were dissolved in household bleach. The replica membranes were mounted on Formvar-filmed grids, immersed in

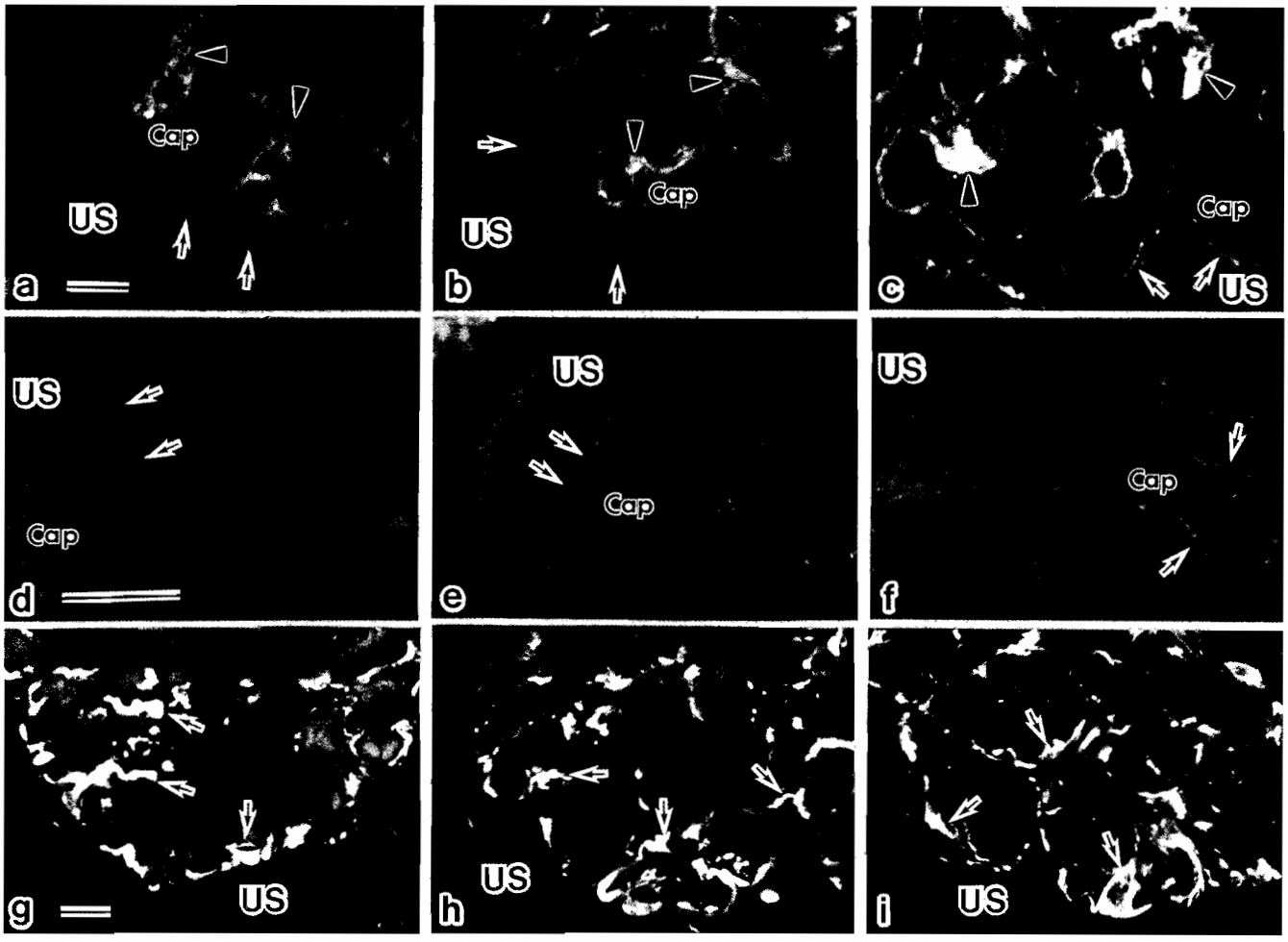

Fig. 2. Immunofluorescence staining of glomeruli in the control (a,d,g), the 6-hr BUO (b,e,h) and the 24-hr BUO (c, f, i) groups observed by confocal laser scanning microscopy. **a-c.** Staining with phalloidin-FITC. Glomerular capillary walls (arrows) and mesangial lesions (arrowheadss). **d-f.** Immunostaining of α-tubulin. The major processes and cell bodies (arrows) of podocytes at high magnification. **g-i.** Immunostaining of vimentin. The perikarya of podocytes are heavily immunostained (arrows). Cap: capillary lumen; US: urinary space. a-c, x 800; d-f, x 1,600; g-i, x 630. Bars: 10 μm.

amyl acetate solution to dissolve the collodion and then examined under a Hitachi H-600 electron microscope at 75kV.

Results

Morphological changes of renal glomeruli stained with hematoxylin-eosin were observed by light microscopy (Fig. 1). In the 6-hr BUO group (Fig. 1b), the size of glomeruli was larger and glomerular capillary tufts were also larger than those of the control group (Fig. 1a). The glomerular capillary seemed to be open. In the 24-hr BUO group, there was also wider expansion of Bowman's space and glomerular tufts with distinctly dilated capillary lumens (Fig. 1c). The distal convoluted tubule in the vascular pole was more widely expanded during the time course of BUO.

The fluorescence staining with phalloidin-FITC showed normal profiles of glomerular capillary loops and mesangial regions in the control group (Fig. 2a). In the 6-hr BUO group, the capillary lumen was also suppressed and the fluorescence intensity around the glomerular basement membrane (GBM) became stronger and the profiles of podocyte cell bodies were slightly observed (Fig. 2b). These changes in the staining pattern became more distinct around the extremely dilated glomerular capillaries in the 24-hr BUO group (Fig. 2c). The immunostaining of tubulin protein was slightly recognized in the podocyte cell bodies and major processes (Fig. 2d). In both 6-hr BUO and 24-hr BUO groups, the immunofluorescence intensity became stronger and the dotted reaction products were distributed linearly in podocytes (Figs. 2e,f). The vimentin protein was also immunologically detected in podocytes, but there was no clear difference in glomeruli between the control and experimental groups (Fig. 2g-i)

As immunostaining controls, the specific immunofluorescence was not identified in the control, and in both 6-hr BUO and 24-hr BUO gorups (data not shown).

The QF-DE method revealed three-dimensional ultrastructures in cell bodies and foot processes of podocytes in the control group (Figs. 3a, 4a). Some

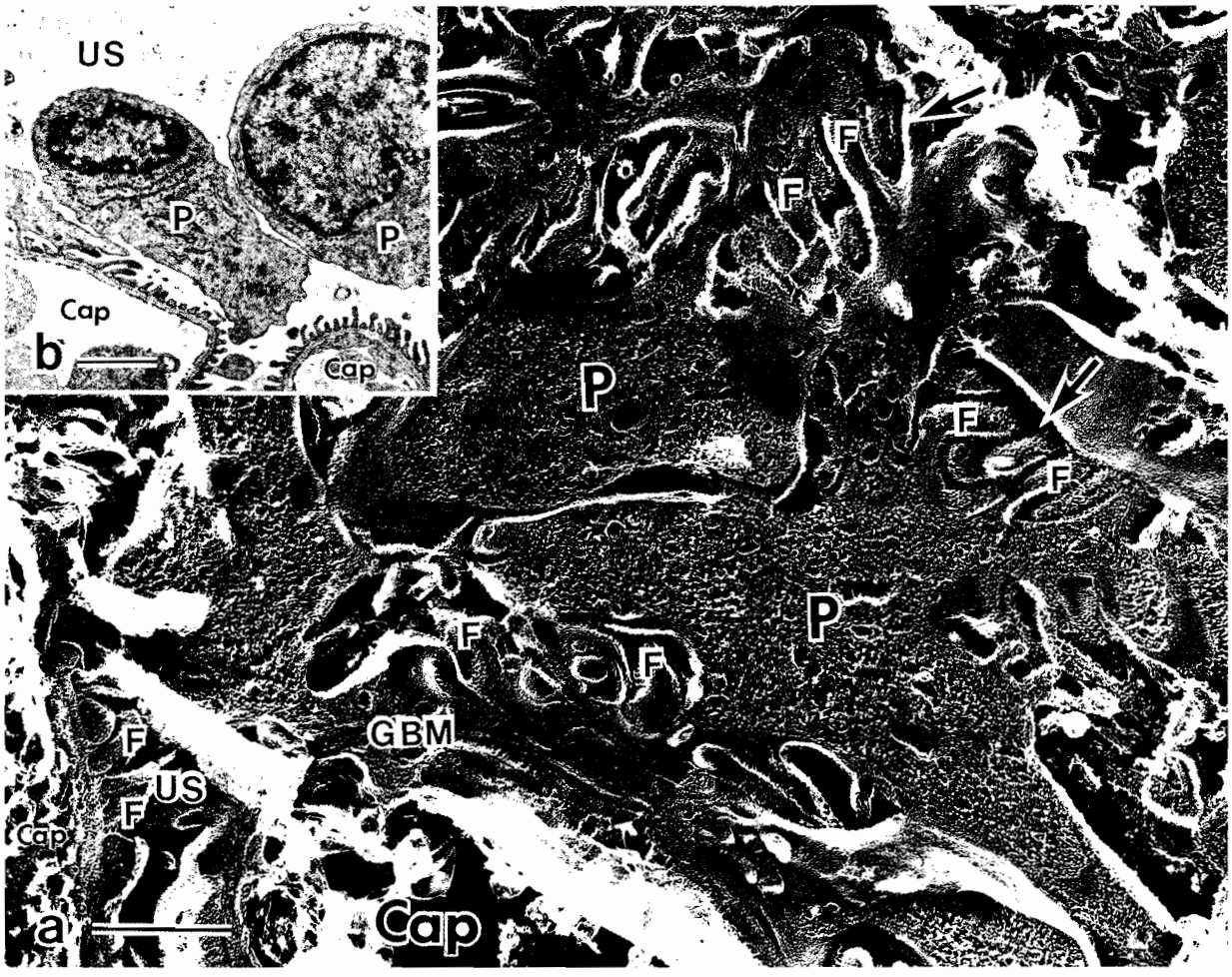

Fig. 3. a. Replica electron micrograph of a glomerulus in the control group. Podocytes with numerous interdigitated foot processes (arrows) along the glomerular capillaries. **b.** Corresponding areas on a conventional ultrathin section. Cap: capillary lumen; US: urinary space; P: podocyte; F: foot process; GBM: glomerular basement membrane. a, x 17,900; b, x 5,000. Bars: 1 μm.

podocytes were located closely, with an interdigitation of their foot processes around glomerular capillaries (Fig. 3a), which were hardly observed with the conventional ultrathin section of the glomerulus (Fig. 3b). The cell body of podocytes was composed of loose networks of cytoskeletons with diameters of 5-25 nm (Fig. 4b). The freeze-fractured capillary loops in the control group were also observed on the replica membrane (Fig. 5a), as compared with their conventional electron micrograph (Fig. 5b). The lamina densa of the GBM was composed of fibrous networks, and the lamina rara externa was composed of fibrils perpendicularly connecting the lamina densa with foot processes. Moreover, the slit diaphragms were observed between foot processes (Fig. 5a).

Fig. 6 illustrates conventional electron micrographs of glomeruli in the 6-hr BUO group. Foot processes became relatively higher and thinner, and their bases attaching to the GBM were less expanded than those in the control group (Fig. 6a,b). The primary processes were stretched, and the profile of the podocyte cell body became more irregular than that in the control group (Fig. 6a).

The replica membranes obtained from the 24-hr BUO group are shown in Figures 7 and 8. The major processes were severely stretched and thinner (Fig. 7a), with the same appearance as observed in the conventional electron micrograph (Fig. 7b). Fibrils with diameters of 5-12 nm were observed, which ran parallel to the cell membrane (Fig. 7a). The foot processes were also stretched, and their cytoplasmic parts attaching to the GBM became narrow. The slit diaphragms between foot processes and the connecting fibers between the lamina densa and the endothelium appeared to be loosely organized (Fig. 8a). In the conventional electron micrograph, not only the fusion of foot processes, but also the cystic formation of podocytes was often observed in the 24-hr BUO group (Fig. 8b).

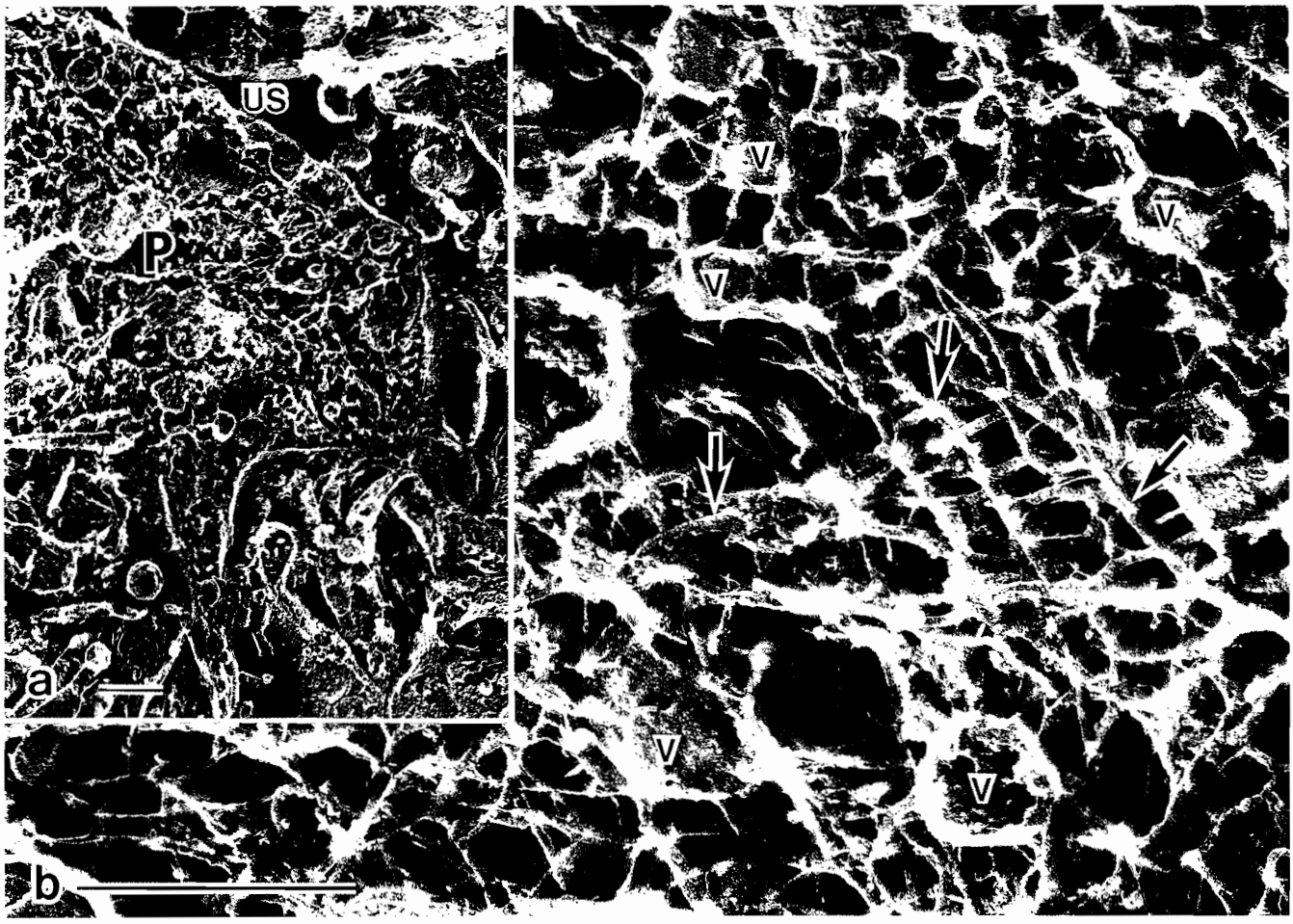

Fig. 4. a. Replica electron micrograph of a glomerulus in the control group. **b.** Highly magnified replica micrograph shows a loose network of fibrils in the cell body of podocytes (arrows).US: urinary space; P: podocyte; MP: major process; GBM: glomerular basement membrane. V: vesicle. a, x 17,600; b, x 78,800. Bars: 0.5 μm.

Discussion

It has been reported that some podocyte damage, which is induced by mechanical stress, is usually observed in animal models under the condition of hyperfiltration (Olson et al., 1985). Such morphological changes of podocytes were also observed in young rats after uninephrectomy (Nagata and Kriz, 1992; Nagata et al., 1992). So the deterioration of glomerular capillary tufts in hyperfiltration is probably caused by mechanical stress to podocytes. The morphological changes of such podocytes develops into serious lesions, eventually initiating a final phase of glomerular sclerosis (Nagata and Kriz, 1992; Nagata et al., 1992). By transmission electron microscopy (TEM) and scanning electron microscopy (SEM), some examinations of rats with uninephrectomy have indicated morphological alterations of podocytes (Nagata and Kriz, 1992; Nagata et al., 1992), which include attenuation of the cell body, vacuole formation, lengthening and stretching of major processes, fusion of foot processes and detachment from the glomerular basement membrane (GBM). Moreover, the detachment of foot processes from the GBM was pointed out to lead to massive proteinuria and to play an important role in glomerular sclerosis (Kanwar and Rosenzweig, 1982). The present study describes similar morphological changes of podocytes, so the podocytes of obstructive kidneys are expected to be under such a similar mechanical stress to those with uninephrectomy (Nagata and Kriz, 1992; Nagata et al., 1992).

The physiological changes in obstructive kidneys have also been reported by several investigators (Purkerson and Klahr, 1989; Klahr and Harris, 1992; Takihana et al., 1994). In animals with BUO intratubular pressures were kept to be increased until 5 hours from the beginning of obstruction. Moreover, there was a progressive increase of renal blood flow in the obstructive kidneys, which peaked at 2-3 hours after an

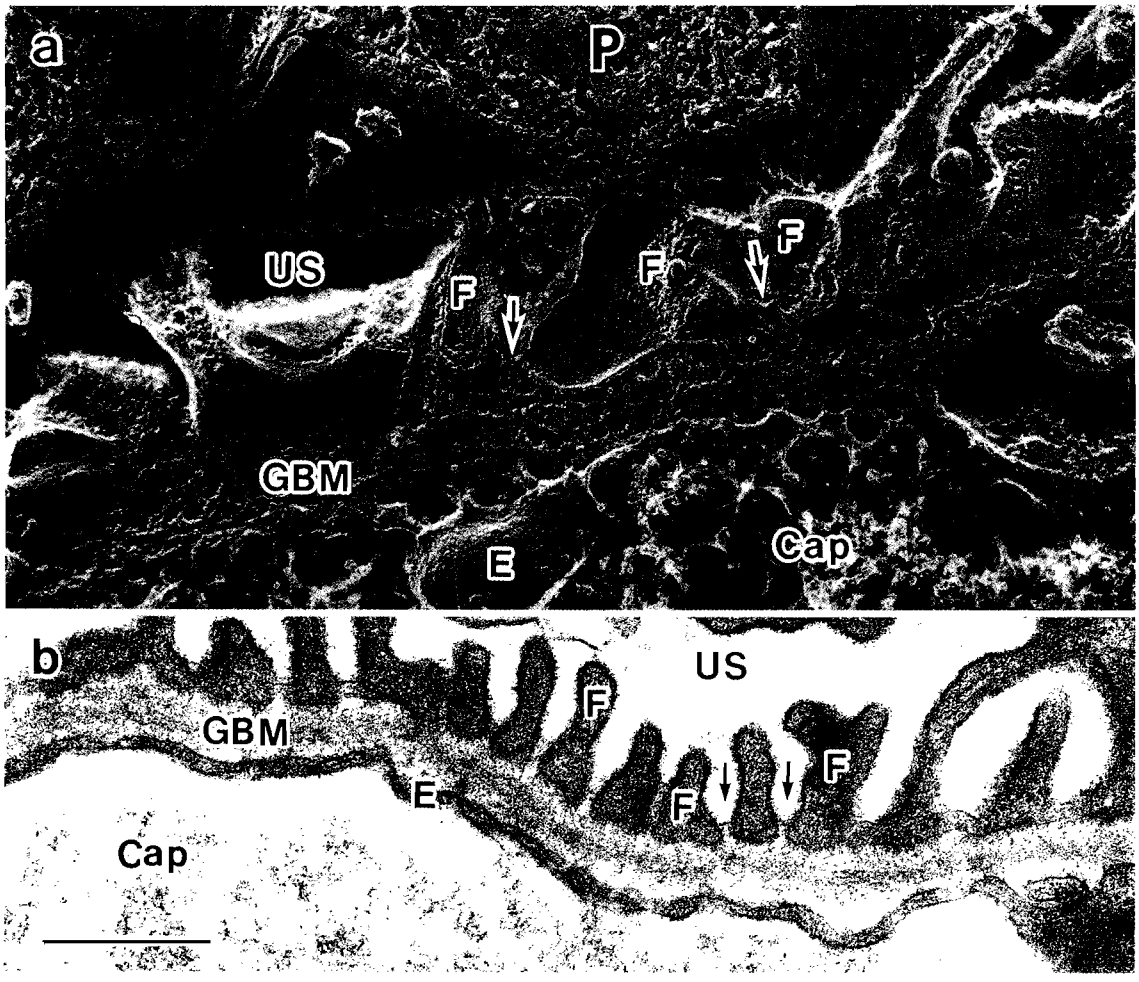

Fig. 5. a. Replica electron micrograph of a glomerular capillary loop in the control group. The glomerular basement membrane contains fibrillary meshworks. The slit diaphragms between foot processes are seen (arrows). **b.** Conventional ultrathin section. The slit diaphragms are observed as thin lines between foot processes (arrows). Cap: capillary lumen; US: urinary space; P: podocyte; F: foot processes; GBM: glomerular basement membrane; E: endothelium. x 43,000. Bars, 0.5 μm.

onset of obstruction. Thereafter, the renal blood flow decreased, so its value is compatible with that obtained prior to ligation of the ureter in 5 hours. Twenty-four hours after the onset of obstruction, the proximal intratubular pressures were decreased, but remained higher than normal values. At this time, the renal blood flow was decreased, because of an increased renal vascular resistance (Klahr and Harris, 1992).

The present study suggests that structural damage of podocytes are more severely induced in the 24-hr BUO group than in the 6-hr BUO group. It has been reported that the renal function in the 6-hr BUO group was well preserved, as compared with that in the 24-hr BUO group (Takihana et al., 1994). These physiological data are well correlated to the present structural changes. So, the glomerular dysfunction is probably associated with the damage of podocytes in the obstructive kidneys. In the present study, both LM and TEM examinations showed that glomerular capillary loops became dilated and capillary tufts were hypertrophied in the 24-hr BUO group much more than in the 6-hr BUO group. This result may indicate that the glomerular capillary pressure in such rabbits is still higher in the 24-hr BUO group than in the control group. It is also suggested that the mechanical stress in the obstructive kidneys may correlate with the difference of relative locations between glomerular capillaries, when the glomerular capillary loops are dilated.

It has been questioned whether or not podocytes respond to pathological conditions in order to prohibit the alterations, including the detachment from the GBM. However, there may be a limitation in the capacity of podocytes for morphological changes, and their weakness is concerned with intracellular cytoskeletons (Andrews, 1988). The cytoskeletons of podocytes are composed of actin filaments, microtubules and intermediate filaments consisting of vimentin protein. Their distribution and physiological roles have been investigated by TEM, SEM and immunofluorescence methods (Bachman et al., 1983; Andrews, 1988; Drenckhahn and Franke, 1988). In these studies, the actin filaments are localized beneath the cell membrane of podocytes, especially in apical parts of foot processes. They are arranged in bundles, either perpendicular or parallel to the GBM. The distribution of myosin proteins is reported to be similar to that of actin filaments. These contractile elements are responsible for morphological alterations, and podocyte foot processes are able to

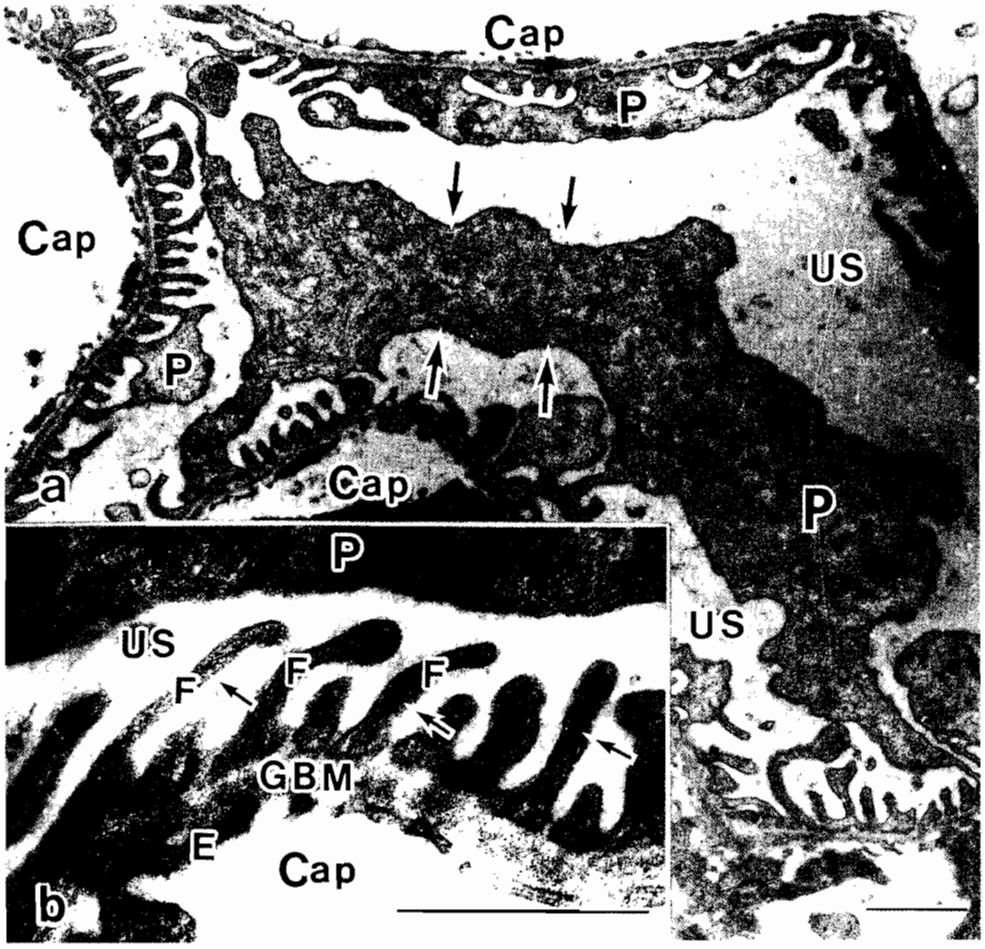

Fig. 6. Electron micrographs of glomeruli in the 6-hr BUO group, as observed on conventional ultrathin sections. **a**. The profile contour of podocytes becomes irregular (arrows), so they seem to be stretched in various directions. **b.** Tall and slender foot processes (arrows) localized along the glomerular basement membrane. Cap: capillary lumen; US: urinary space; P: podocyte; F: foot process; GBM: glomerular basement membrane. E; endothelium. a, x 11,600; b, x 37,500. Bars: 1 μm.

retract under some pathological conditions (Andrews, 1988). In this study, the phalloidin-FITC was used for fluorescence staining for actin filaments. It was demonstrated that actin filaments were concentrated in foot processes and also under the cell membrane of cell bodies and major processes in both experimental groups of BUO. This is probably because an increase of actin filaments reinforces the connection between foot processes and the GBM to prevent the detachment from the GBM, which usually initiates and promotes glomerular sclerosis (Andrews, 1988). Especially, such an increase of actin filaments in cell bodies and major processes means that the have a capacity to maintain the structural integrity of podocytes.

Microtubules usually existed in the cell body of podocytes, where they were separated from each other or clustered into bundles. In major processes, bundles of microtubules ran parallel to the long axis of processes. Such microtubules are thought to be important for maintaining the structural integrity of the cell body and major processes (Andrews, 1988; Dreckhahn and Franke, 1988). The present immunofluorescence study demonstrates the morphological changes of microtubules during the time course of BUO. It is suggested that such microtubules in BUO are bundled to resist the mechanical tension and to maintain the structural integrity of podocytes, and also probably have transport functions as in nerve fibers (Andrews, 1988; Dreckhahn and Franke, 1988). Moreover, it was demonstrated that numerous intermediate filaments existed in the cell body and major processes which formed networks. So they are assumed to be main cytoskeletons, which maintain the structural integrity of podocytes rather than the microtubules. It is concluded that the ultrastructural study of podocytes with CLSM and QF-DE methods is useful to check morphological changes, corresponding to the post-obstructive renal function.

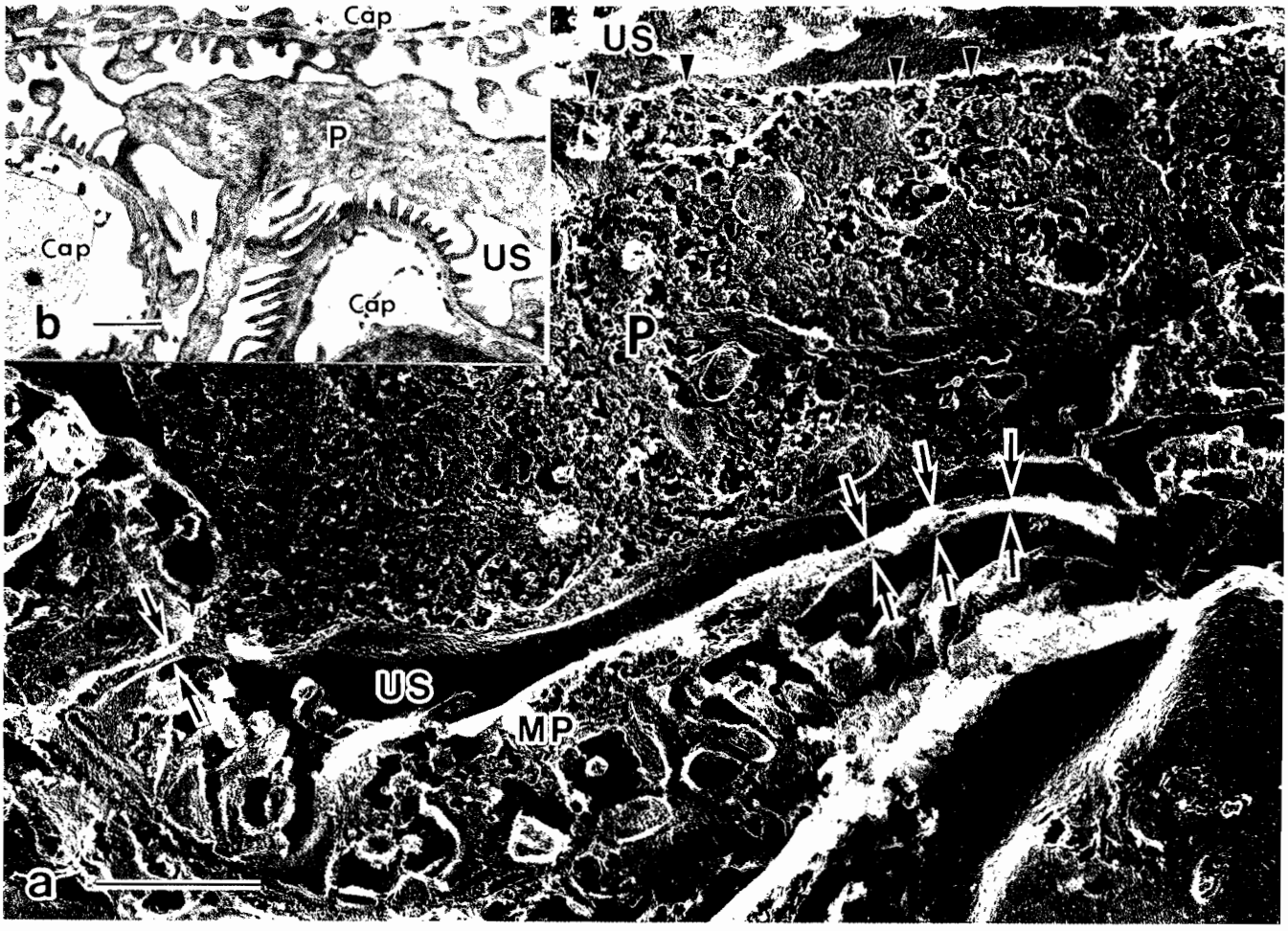

Fig. 7. Electron micrographs of glomeruli in the 24-hr BUO group. **a.** Replica electron micrograph of a glomerulus. A podocyte is so stretched that its major processes are flattened and narrow (arrows). Fibrils, which run parallel to the cell membrane of the podocyte, are clearly identified (arrowheads). **b.** Corresponding areas on a conventional ultrathin section. Cap: capillary lumen; US: urinary space; P: podocyte; MP: major processes. a, x 22,900; b, x 7,000. Bars, 1 μm.

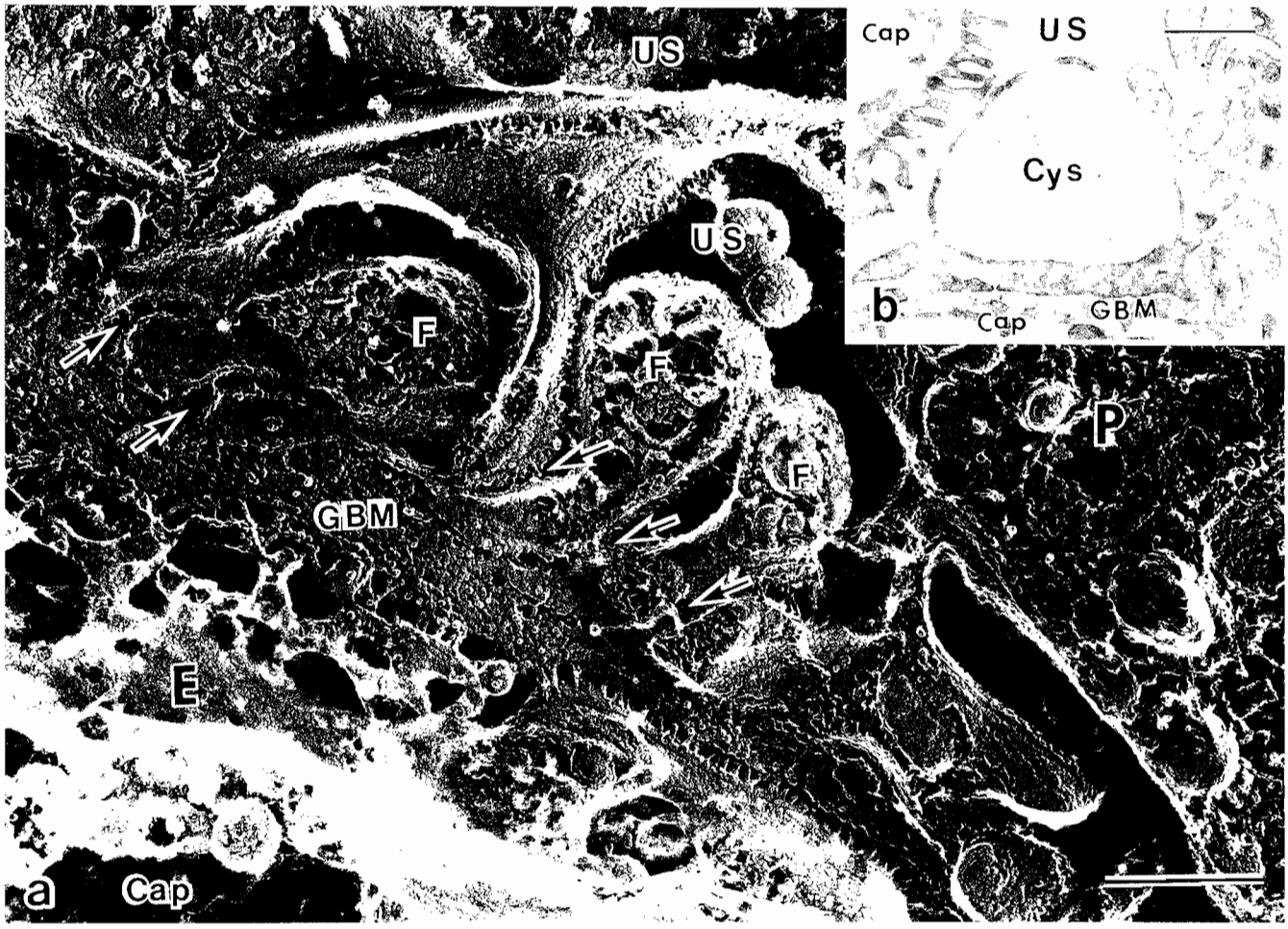

Fig. 8. Electron micrographs of glomeruli in the 24-hr BUO group. **a.** The slit diaphragms between foot processes become loosely arranged (arrows), and the connecting fibrils between the lamina densa and the endothelium have a partly deficit (arrowheads). **b.** Conventional ultrathin section. There is a cystic formation in the process of a podocyte. Cap: capillary lumen; US: urinary space; P: podocyte; F: foot process; GBM: glomerular basement membrane; E: endothelium; Cys: cystic formation. a, x 43,000; b, x 12,000. Bars, 0.5 μm.

Acknowledgements. The authors are grateful to Miss Y. Kato for her excellent technical assistance.

References

Andrews P.M. (1988). Morphological alteration of the glomerular (visceral) epithelium in response to pathological and experimental situations. J. Electron Microsc. Tech. 9, 115-144.

Bachmann S., Kriz W., Kuhn C. and Franke W.W. (1983). Differentiation of cell types in the mammalian kidney by immunofluorescence microscopy using antibodies to intermediate filament proteins and desmoplakins. Histochem. 77, 365-394.

Dreckhahn D. and Franke R.P. (1988). Ultrastructural organization of contractile and cytoskeletal proteins in glomerular podocytes of chicken, rat, and man. Lab. Invest. 59, 673-682.

Elema J.D. and Arends A. (1975). Focal and segmental glomerular hyalinosis and sclerosis in the rat. Lab. Invest. 33, 554-561.

Frise J.W.U., Standstrom D.J., Meyer T.W. and Rennke H.G. (1989). Glomerular hypertrophy and epithelial cell injury modulate progressive glomerulosclerosis in the rat. Lab. Invest. 60, 205-218.

Kamiya S. (1968). Electron microscopic study on experimental uremic rat kidney by bilateral ureteral ligation. Jpn. J. Urol. 59, 941-961.

Kanwar S.Y. and Rosenzweig L. (1982). Altered glomerular permeability as a result of focal detachment of the visceral epithelium. Kidney Int. 21, 565-574.

Klahr S. and Harris K.P.G. (1992). Obstructive uropathy. In: The kidney. Physiology and pathophysiology. Seldin and Giebisch (eds). Raven Press. New York. pp 3327-3369.

McDougal W.S. (1990). Pathophysiology of glomerular dysfunction following ureteral obstruction. Dialogues Pediatr. Urol. 13, 7-8.

Nagata M. and Kriz W. (1992). Glomerular damage after uninephrectomy in young rats. II. Mechanical stress on podocytes as a pathway to sclerosis. Kidney Int. 42, 148-160.

Nagata M., Schärer K. and Kriz W. (1992). Glomerular damage after uninephrectomy in young rats. I. Hypertrophy and distortion of capillary architecture. Kidney Int. 42. 136-147.

Nagle R.B. and Bulger R.E. (1978). Unilateral obstructive nephropathy in the rabbit. II. Late morphologic changes. Lab. Invest. 38, 270-278.

Nagle R.B., Bulger R.E., Cutler R.E., Jervis H.R. and Benditt E.P. (1973). Unilateral obstructive nephropathy in the rabbit. I. Early morphologic, physiologic, and histochemical changes. Lab. Invest. 28, 456-467.

Naramoto A., Ohno S., Itoh N., Shibata N., Nakazawa K., Takami H., Duan H.J., Kasahara H. and Sigematsu H. (1991a). Ultrastructural study of matriceal changes in chronic phase of Masugi nephritis by quick-freezing and deep-etching method. Virchows Arch. (A) 418, 51-59.

Naramoto A., Ohno S., Itoh N. and Sigematsu H. (1991b). Three-dimensional ultrastructure of glomerular injury in serum sickness nephritis using the quick-freezing and deep-etching method. Virchows Arch. (A) 418, 185-192.

Ohno S., Hora K., Furukawa T. and Oguchi H. (1992). Ultrastructural study of the glomerular slit diaphragm in fresh unfixed kidney by a quick-freezing method. Virchows Arch. (B) 61, 351-358.

Olson J.L., Urdaneta A.G. and Heptinstall R.H. (1985). Glomerular hyalinosis and its relation to hyperfiltration. Lab. Invest. 52, 387-398.

Purkerson M.L. and Klahr S. (1989). Prior inhibition of vasoconstrictor normalizes GFR in postobstructed kidney. Kidney Int. 35, 1306-1314.

Takihana Y., Tago K. and Ueno A. (1994). Renal function reserve in obstructive nephropathy. Jpn. J. Nephrol. 36, 130-137.

White J.C., Amos W.B. and Fordham M. (1987). An evaluation of confocal versus conventional imaging of biological structures by fluorescence light microscopy. J. Cell Biol. 105, 41-48.

Accepted September 1, 1997